Atomic-layer Dependence of Shear Modulus in Two-dimensional Single-crystal Perovskites

Qikun Li,[1,2] Sheng Bi,[1,2] Jingyuan Bu,[1] Qinglei Guo,[3] Chaolong Tang,[4]

Zhongliang Ouyang,[5] Chengming Jiang[1,2],* and Jinhui Song[1,2],*

*E-mail: jiangcm@dlut.edu.cn and jhsong@dlut.edu.cn

SUPPORTING INFORMATION

SECTION 1: The lateral force analysis of AFM

When the dimensions of the cantilever are obtained, the lateral spring constants k_l can be calculated from[1]

$$k_l = \frac{Gwt^3}{3l(h+t/2)^2} \qquad (S1)$$

where G is the cantilever shear modulus, w, t, l and h are the width, thickness, length and tip height of the AFM cantilever, respectively

The photodiode sensitivity is defined as the ratio of the photodiode voltage and the deflection of the AFM cantilever

$$S_l = \frac{V_l}{x_l} \qquad (S2)$$

where S_l is the lateral deflections sensitivity of the cantilever, V_l is the corresponding photodiode voltage output and the x_l is the deformation in lateral direction.

For cantilever with rectangle cross section, the lateral force F_l can be expressed as

$$F_l = \frac{k_l}{S_l} V_l = \alpha V_l \qquad (S3)$$

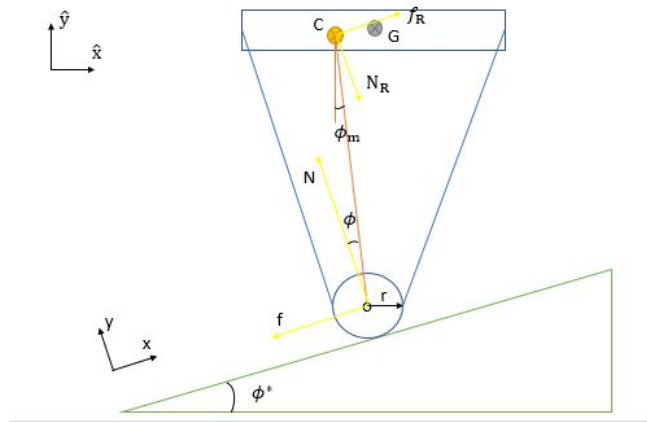where α is defined as the transition coefficient, and V_l is the corresponding photodiode voltage output.

Figure S1. The cross-section schematic of the tip in contact mode

Actually, α is also calibrated by the α_{ln} and α_{ll} [2,3] as shown in figure S1, and the

calibrated transition coefficient can be expressed as

$$\alpha_{ll} = \alpha_l[(1-\gamma)\cos\phi_m + \gamma\cos\phi^*] \qquad (S4)$$

$$\alpha_{ln} = \alpha_n \frac{(1-\gamma)\sin\phi_m + \gamma\sin\phi^*}{(1-\gamma)\cos\phi_m + \gamma\cos\phi^*} \qquad (S5)$$

where α_n is the transition constant in the normal direction; α_{ll} is the transition

constant in lateral direction; and α_{ln} is the interference transition constant in

lateral direction; and the γ is r/(h+r). The lateral force can be expressed as

$f = \alpha_{ll}V_l + \alpha_{ln}V_n$

It is noticed that α_{ll}, α_{ln} equals to α_l when ϕ_m and ϕ^* equal to 0.

SECTION 2: Synthesis and microfabrication of the 2D hybrid perovskites[4,5]

10 mL butylamine and 20 mL methanol were added into a 250 mL round bottom flask. Then the mixture was stirred and maintained using an ice-water bath. Meanwhile, 10 mL 50 wt% HBr was dissolved in water and then further was added to the mixture drop by drop. Then the solution was placed at room temperature and stirred for at least 3 hours. The solvent was removed by a rotary evaporator at 60 °C and the crude oil-like material was obtained, which was then washed with diethyl ether three times by stirring the solution for 40 min. After recrystallization and filtration, $C_4H_9NH_3Br$ precursor, the white solid material, was collected and dried at 50 °C in vacuum for 24 hours.

Inside a nitrogen-filled glove box, which the level of oxygen and water were controlled to be less than 1 ppm, 1 mmol as-synthesized $C_4H_9NH_3Br$ and 0.5 mmol $PbBr_2$ were dissolved in DMF/chlorobenzene co-solvent with volume ratio 1:1 and diluted to be 5mM in a 100mL volumetric flask. Furthermore, the solution was diluted to 0.075mM by 2:1 chlorobenzene/acetonitrile co-solvent.

$(C_4H_9NH_3)_2PbBr_4$ was grown on the Si substrate coated with 300nm-thick SiO_2. The SiO_2/Si substrates were cleaned in deionized water, isopropanol, acetone, deionized water for 5min in sequence, and then dried by nitrogen and cleaned in Harrick plasma O_2 plasma cleaner with high power for 10min. Then the growth process was carried out in glove box.

The cleaned substrate was preheated at 60 °C on a hot plate, and 20uL prepared $(C_4H_9NH_3)_2PbBr_4$ solution was dropped onto the substrate and dried at 60 °C for 10 min for solvent evaporation. The sheet-like crystals were grown on SiO_2/Si substrate, and then were attached to a regular scotch tape. The tape with the crystals was placed on shiny-side of another cleaned substrate and keep it in 120°C. Then the tape was gently removed and the substrate was washed in hexanes again. The sample was dried at 60 °C for 10 min. The area of the substrate with 2D perovskite was measured by AFM with non-contact mode, meanwhile the height and size were recorded. The desired sample was marked for further measurement. As shown in Figure S1, the sample was fabricated on SiO_2/Si substrate and the 2μm ×2μm 2D perovskites with different height were marked by AFM.
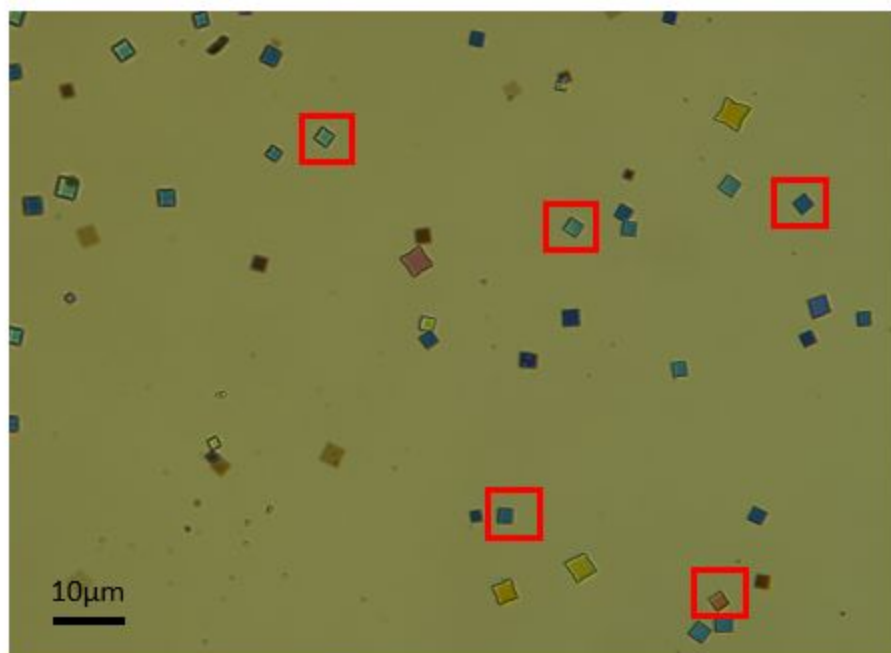
Figure S2. 2D perovskites fabricated on SiO_2/Si substrate, the 2μm $\times$ 2μm size with different height were marked with red boxes

SECTION 3: The van der Waals interaction

The basic physics of van der Waals force can be understood from a simple one-dimension layered model of $\mathcal{H}_0$ consisting of electrons bounded by harmonic oscillator forces and $\mathcal{H}_1$ consisting of Coulomb interactions between the dipoles[6]

$$\mathcal{H} = \mathcal{H}_0 + \mathcal{H}_1 \tag{S6}$$

where the

$$\mathcal{H}_0 = \frac{1}{2m}P_1^2 + \frac{1}{2}m\omega_0^2 x_1^2 + \frac{1}{2m}P_2^2 + \frac{1}{2}m\omega_0^2 x_2^2$$

$$\mathcal{H}_1 = \frac{e^2}{4\pi}\left(\frac{1}{R} + \frac{1}{R+x_1-x_2} - \frac{1}{R+x_1} - \frac{1}{R-x_2}\right) \tag{S7}$$

and R is the length between the layers, m is the effective mass and x_1, x_2 are the length of charge separation. Assuming that the separation of layer charges is large compared to the size of the atom $(R \gg x_1, x_2)$, $\mathcal{H}_1$ can be approximately simplified as

$$\mathcal{H}_1 \approx -2\frac{e^2 x_1 x_2}{4\pi R^3} \tag{S8}$$

and the system, expressed as Eq.(S6), can be diagonalized in terms of coordinates $x_\pm = (x_1 \pm x_2)/\sqrt{2}$

$$\mathcal{H} = \frac{P_+^2}{2m} + \frac{1}{2}\left(m\omega_0^2 - \frac{2e^2}{4\pi R^3}\right)x_+^2 + \frac{P_-^2}{2m} + \frac{1}{2}\left(m\omega_0^2 - \frac{2e^2}{4\pi R^3}\right)x_-^2 \tag{S9}$$

It's obvious that in terms of independent harmonic oscillators is $\omega_\pm$ in coordinates $x_\pm$, which can be considered as the ω_0 with the shifted frequencies, shown in Eq.(S9)

$$\omega_\pm = \sqrt{\omega_0^2 \mp \frac{2e^2}{4\pi m R^3}} \cong \omega_0 \mp \frac{e^2}{4\pi m\omega_0 R^3} - \frac{e^4}{32\pi^2 m^2 \omega_0^3 R^6} + \cdots \tag{S10}$$

The van der Waals potential is simply the shift in the ground state (zero point) energy due to the Coulomb interaction, and is found to be

$$V(R) = \frac{1}{2}\omega_+ + \frac{1}{2}\omega_- - 2\left(\frac{1}{2}\omega_0\right) \cong -\frac{e^4}{32\pi^2 m^2 \omega_0^3 R^6} \tag{S11}$$

In "London" form, the van der Waals interaction is:

$$\Delta E_{vdW} \cong -\frac{B}{R^6}$$

(S12)

where B is the coefficient of the attraction interaction. The repulsion interaction, which is usually expressed as $-\frac{A}{R^{12}}$, can be neglectable as Eq(S8) shown.

As a result of the atomic layer depending shear modulus stated in context, we have further studied the interaction and the modified surface layers. The Hamiltonian of the system, which does not consider the screening effect of adjacent layers dipoles, can be expressed as
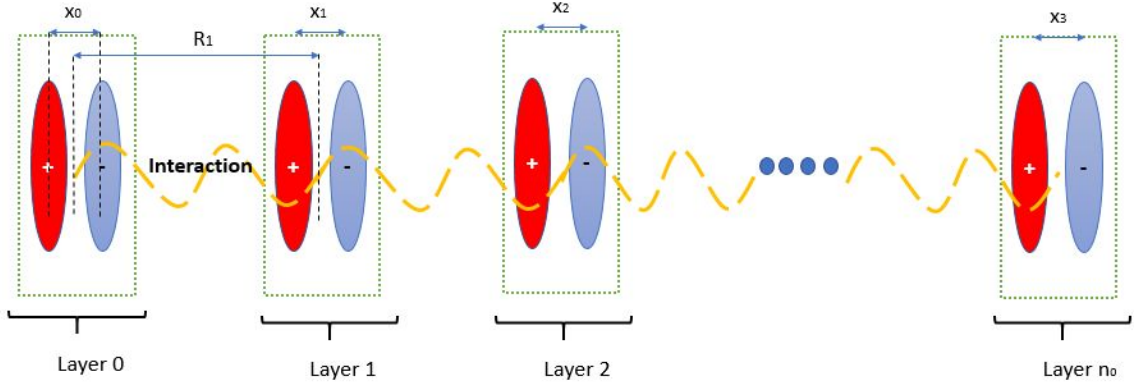

Figure S3. Sketch map of 2D perovskites interaction model

$$\mathcal{H} = \sum_{i=0}^{n_0} \mathcal{H}_i = \sum_{i=0}^{n_0-1}\left(\frac{1}{2m}P_i^2 + \frac{1}{2}m\omega_i^2 x_i^2\right) + \sum_{i=1}^{n_0-1}\left[\frac{e^2}{4\pi}\left(\frac{1}{R_i} + \frac{1}{R_i+x_i-x_{i+1}} - \frac{1}{R_i+x_i} - \frac{1}{R_i-x_{i+1}}\right)\right]$$

(S13)

where $\mathcal{H}_i$ is Hamilton of the 2D perovskites consisting of electrons bounded by harmonic oscillator forces and Coulomb interactions of layer i depending on the actual interaction length between layers as figure S3 shown, and n_0 is the total number of sample layers.

Actually, the 2D perovskites can be treated as a composite film with a sandwich structure, which possesses inner and outer layers. It is noticed that the surface effect extending into the bulk is a gradual process and fades off slowly. To simplify, the outer surface layers are approximately regarded as a uniform shell possessing an average bond contraction with an interaction length r_s, and inner layers as a uniform layer with an interaction length r_0. $\mathcal{H}$ can be sorted out as

$$\mathcal{H} \cong \sum_{i=0}^{n_s} \left[\frac{1}{2m} P_i^2 + \frac{1}{2} m \left(\omega_i^2 - \frac{e^2}{\pi m r_s^3} \right) x_i^2 \right] + \sum_{i=n_0-n_s}^{n_0} \left[\frac{1}{2m} P_i^2 + \frac{1}{2} m \left(\omega_i^2 - \frac{e^2}{\pi m r_s^3} \right) x_i^2 \right] + \sum_{i=n_s+1}^{n_0-n_s-1} \left[\frac{1}{2m} P_i^2 + \frac{1}{2} m \left(\omega_i^2 - \frac{e^2}{\pi m r_0^3} \right) x_i^2 \right] - C$$

(S14)

where C is a compensation term and $x_i x_{i+1} \cong x_i^2$. The wave function is approximated as $\varphi(\mathbf{x}) = \varphi(x_1)\varphi(x_1)\varphi(x_2)\cdots$, van der Waals potential which is the shift in the ground state (zero point) energy by Coulomb interaction can be expressed as

$$V(R) \cong \sum \left(\frac{1}{2} \omega_\pm - \frac{1}{2} \omega_i \right) + c = -\frac{e^4}{32\pi^2 m^2 \omega_0^3} \left(\frac{n_0}{r_s^6} + \frac{n_0 - n_s}{r_0^6} \right) + c \quad \text{(S15)}$$

We can obtain the formula with the correction factor described as following:

$$\Delta E_{vdW} \cong -\frac{B}{r_0^6} \left[1 + \frac{\left(\frac{r_s}{r_0}^{-6} - 1 \right) n_s}{n_0} \right] + c \quad \text{(S16)}$$

SECTION 4: The shear modulus of 2D perovskites

The Linear Elastic Model

The Linear Elastic model is used to describe materials in the situation:

(1) the strains are small
(2) the stress is proportional to the strain $\sigma \propto \varepsilon$
(3) there is no dependence on the rate of loading or straining

Figure S4 shows the first scan and the tenth repeated scan by the red and blue lines in the topography. The figure S4 shown that the deformation of 2D perovskites is elastic.
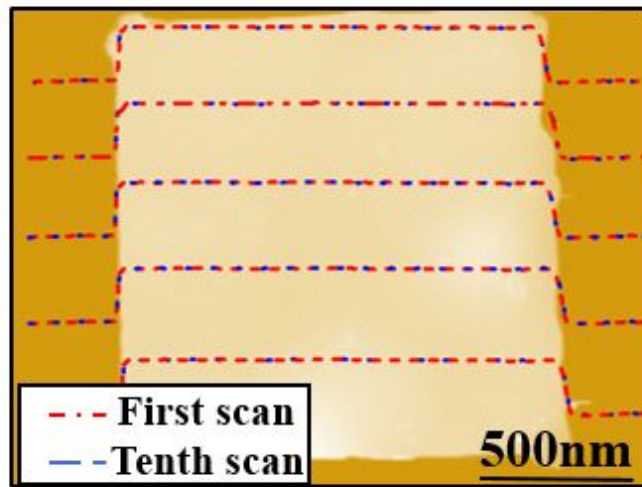

Figure S4. The data line of the first scan and the tenth repeated scan

Anisotropic Elasticity

It is needed to discuss Hooke's Law for anisotropic cases in general. In general three-dimension case, there are six components of stress and the corresponding six components of strain. In general cases, Hooke's law may be expressed as:

$$\varepsilon_i = S_{ij}\sigma_j \tag{S177}$$

where S_{ij} is compliant coefficient tensor. Expansion of Eq. S15 will produce nine equations. Hooke's law can be written as

$$\varepsilon_{ij} = S_{ijkl}\sigma_{kl} \tag{S18}$$

S_{ijkl} are fourth-rank tensor quantities with 81 constants in all. It is important to note that both σ_{ij} and ε_{ij} are symmetric tensors, which means that the off-diagonal components are equal. The stress and strain tensor can be written as

$$\begin{pmatrix} \sigma_1 & \sigma_6 & \sigma_5 \\ \sigma_6 & \sigma_2 & \sigma_4 \\ \sigma_5 & \sigma_4 & \sigma_3 \end{pmatrix} and \begin{pmatrix} \varepsilon_1 & \frac{\varepsilon_6}{2} & \frac{\varepsilon_5}{2} \\ \frac{\varepsilon_6}{2} & \varepsilon_2 & \frac{\varepsilon_4}{2} \\ \frac{\varepsilon_5}{2} & \frac{\varepsilon_4}{2} & \varepsilon_3 \end{pmatrix} \tag{S19}$$

In which index can be defined as

$$\begin{pmatrix} 11 & 12 & 13 \\ & 22 & 23 \\ & & 33 \end{pmatrix} = \begin{pmatrix} 1 & 6 & 5 \\ & 2 & 4 \\ & & 3 \end{pmatrix} \tag{S20}$$

It should be noted that $\varepsilon_4 = 2\varepsilon_{23} = \gamma_{23}$, $\varepsilon_5 = 2\varepsilon_{13} = \gamma_{13}$, $\varepsilon_4 = 2\varepsilon_{12} = \gamma_{12}$.

The Hook's law can be express as the general form with the stress and strain as

$$\begin{pmatrix} \varepsilon_1 \\ \varepsilon_2 \\ \varepsilon_3 \\ \varepsilon_4 \\ \varepsilon_5 \\ \varepsilon_6 \end{pmatrix} = \begin{pmatrix} S_{11} & S_{12} & S_{13} & S_{14} & S_{15} & S_{16} \\ S_{21} & S_{22} & S_{23} & S_{24} & S_{25} & S_{26} \\ S_{31} & S_{32} & S_{33} & S_{34} & S_{35} & S_{36} \\ S_{41} & S_{42} & S_{43} & S_{44} & S_{45} & S_{46} \\ S_{51} & S_{52} & S_{52} & S_{54} & S_{55} & S_{56} \\ S_{61} & S_{62} & S_{63} & S_{64} & S_{65} & S_{66} \end{pmatrix} \begin{pmatrix} \sigma_1 \\ \sigma_2 \\ \sigma_3 \\ \sigma_4 \\ \sigma_5 \\ \sigma_6 \end{pmatrix} \tag{S21}$$

Stress-strain relationship can be further simplified by considering the symmetry. The symmetry in compliance matrices requires:

$$S_{ij} = S_{ji} \tag{S22}$$

The 21 independent elastic constants can be reduced by further considering the symmetry conditions found in different crystal structures. Tetragonal has the fourfold rotation around [001]. In terms of a compliance matrix, laminated composites of 2D perovskite have tetragonal symmetry with nine independent elastic constants (for classes 4mm, $\overline{4}$2m,422,4/mmm).

$$\begin{pmatrix} 11 & 12 & 13 & 0 & 0 & 0 \\ & 11 & 13 & 0 & 0 & 0 \\ & & 33 & 0 & 0 & 0 \\ & & & 44 & 0 & 0 \\ & & & & 44 & 0 \\ & & & & & 66 \end{pmatrix} \tag{S23}$$

The simplification of the Hooke's law can be written from the above analysis

$$\begin{pmatrix} \varepsilon_1 \\ \varepsilon_2 \\ \varepsilon_3 \\ \varepsilon_4 \\ \varepsilon_5 \\ \varepsilon_6 \end{pmatrix} = \begin{pmatrix} 1/E_1 & -v_{21}/E_2 & -v_{31}/E_3 & 0 & 0 & 0 \\ & 1/E_2 & -v_{32}/E_3 & 0 & 0 & 0 \\ & & 1/E_3 & 0 & 0 & 0 \\ & & & 1/2G_{23} & 0 & 0 \\ & & & & 1/2G_{13} & 0 \\ & & & & & 1/2G_{12} \end{pmatrix} \begin{pmatrix} \sigma_1 \\ \sigma_2 \\ \sigma_3 \\ \sigma_4 \\ \sigma_5 \\ \sigma_6 \end{pmatrix} \tag{S24}$$

where E is the Young's modulus (stiffness) of the material in corresponding direction, v is the Poisson's ratio representing the ratio of a transverse strain to the applied strain in uniaxial tension, G is the shear modulus representing the shear stiffness in the corresponding plane, and $v_{12} = v_{21}$, $v_{31} = v_{32} = v_{23} = v_{13}$, $G_{32} = G_{32}$, $E_1 = E_2$. The equation can be further expressed as

$$\begin{pmatrix} \varepsilon_{11} \\ \varepsilon_{22} \\ \varepsilon_{33} \\ \varepsilon_{23} \\ \varepsilon_{13} \\ \varepsilon_{12} \end{pmatrix} = \begin{pmatrix} 1/E_1 & -v_{12}/E_1 & -v_{23}/E_3 & 0 & 0 & 0 \\ & 1/E_1 & -v_{23}/E_3 & 0 & 0 & 0 \\ & & 1/E_3 & 0 & 0 & 0 \\ & & & 1/G_{13} & 0 & 0 \\ & & & & 1/G_{13} & 0 \\ & & & & & 1/G_{12} \end{pmatrix} \begin{pmatrix} \sigma_{11} \\ \sigma_{22} \\ \sigma_{33} \\ \sigma_{23} \\ \sigma_{13} \\ \sigma_{12} \end{pmatrix} \tag{S25}$$

According to tetragonal symmetry analysis of the 2D perovskites, the shear modulus in x-y plane can be expressed as:

$$G_{12} = \frac{\tau_{xy}}{\gamma_{xy}} = \frac{\sigma_6}{2\varepsilon_6} = \frac{\sigma_{12}}{\varepsilon_{12}} = \frac{HF}{A\Delta x} \tag{S26}$$

where $\tau_{xy} = F/A$ is the shear stress, F is the domain force, A is the area on which the force is applied, γ_{xy} is the shear strain, Δx is the transverse displacement, H is the initial length. Actually, G in nanoscale needs to be corrected by the analysis in section 3, which can be expressed as

$$G'_{12} = G_{12}\left(1 + \frac{\left(\left(\frac{r_s}{r_0}\right)^{-6} - 1\right)n_0}{n}\right) + c \tag{S27}$$

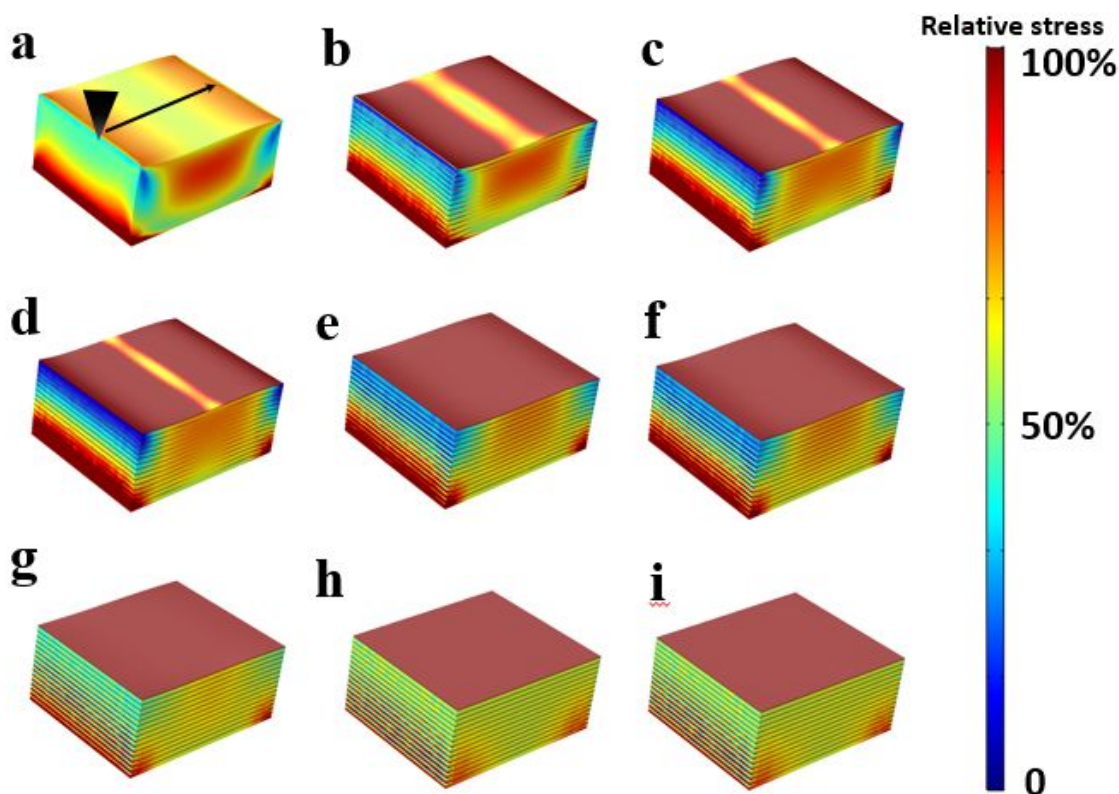SECTION 5: The simulation of layered 2D perovskites

Figure S5. The simulation of layered structure with layered mechanical properties

shear deformation with the lateral force applied

The atomic-layer dependence of shear modulus in 2D $(C_4H_9NH_3)_2PbBr_4$ perovskites was systematically studied by COMSOL. It is noticed that the crystal structure of 2D $(C_4H_9NH_3)_2PbBr_4$ perovskites, with only one atomic-layer of $PbBr_4^{2-}$ separated by organic chains, are held together by weak van der Waals forces. In each 2D atomic-layer, the strong ion bond of $PbBr_4^{2-}$ is much larger than the weak van der Waals forces that links each atomic-layer of $PbBr_4^{2-}$. The corresponding simulation results are obtained by the setting ratio of shear modulus for $PbBr_4^{2-}$ layer and $C_4H_9NH_3$ layer (1:1, 1:5, 1:10, 1:20, 1:50, 1:100, 1:200, 1:500, 1:1000) with the lateral force of 500μN applied to the center of the left edge.

As shown in Figure S2, the stress distribution of 2D perovskite under the lateral force trends to uniformly exert for nanometer thin layer when the ratio of shear modulus larger than 1:200.
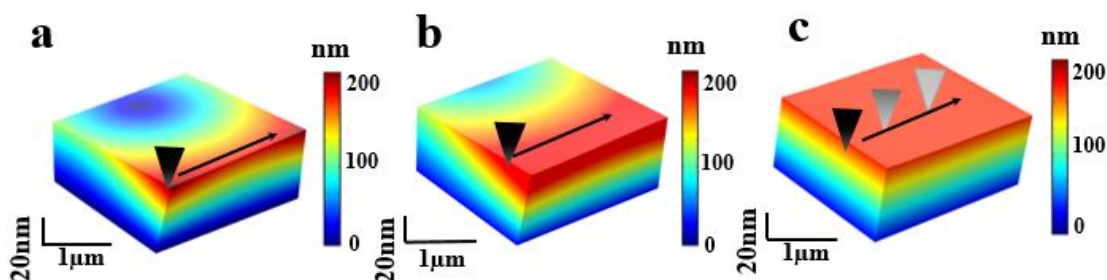

Figure S6. The simulation of shear deformation with the lateral force applied to the vertex, quarter and center of the one edge

To avoid twisted error, the simulations are further investigated by numerical modeling using COMSOL. The points of lateral force are set at the vertex, quarter and center of one edge. As shown in Figure S3, the twisted deformation decreases obviously with the lateral force moving to center of the left edge. And the persistent shear deformation processes stably when the lateral force is applied on the surface.

SECTION6: The measured shear modulus of layered 2D perovskites in 9nN lateral force

Table S1. Measured Shear Modulus of 2D ($C_4H_9NH_3)_2PbBr_4$ Perovskites

Serial number	Area (μm^2)	Height (nm)	Lateral force (μN)	Deformation (nm)	Shear modulus (MPa)
1	3.98	39.8	369.72	89.7	41.22
2	4.42	41.2	355.49	77.4	42.81
3	3.98	41.6	376.63	88.8	44.33
4	3.81	40.4	265.95	68.1	41.41
5	4.24	41.2	342.84	87.7	37.99
6	3.73	41.1	304.57	78.9	42.53
7	3.63	39.2	307.16	69.5	47.73
8	4.32	42.8	284.72	74.4	37.91
9	4.73	40.8	367.63	83.8	37.84

   The Table S1 shows some others measurements at 9nN normal force and the shear modulus characterized at 41.6 ± 3.3 MPa.

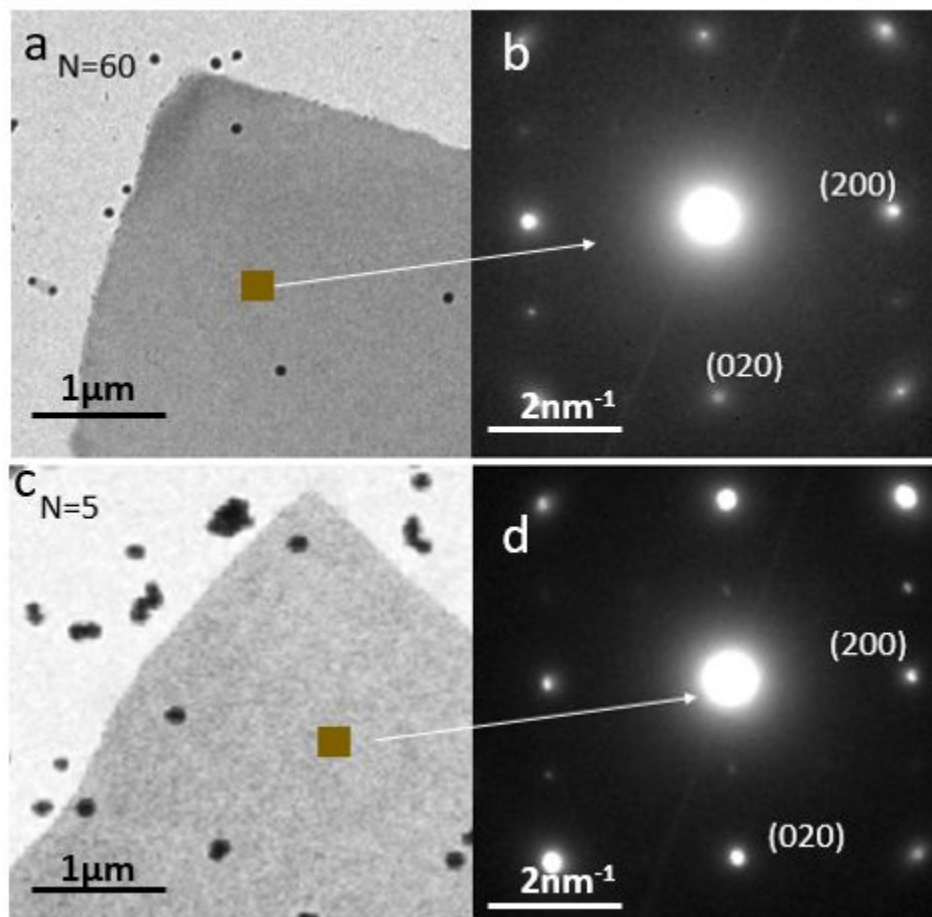SECTION7: The TEM diffraction pattern image of the 2D perovskites

Figure S7. The TEM diffraction pattern image of the 2D perovskites, $(C_4H_9NH_3)_2PbBr_4$.
Figure a and b are the TEM and corresponding diffraction images of a 2D perovskite with 60
layers; Figure c and d are the TEM and corresponding diffraction images of a 2D perovskite with
5 layers.

References:

(1) Xie, H.; Vitard, J.; Haliyo, S.; Régnier, S.; Boukallel, M. Calibration of Lateral Force Measurements in Atomic Force Microscopy with a Piezoresistive Force Sensor. *Rev. Sci. Instrum.* **2008**, *79* (3), 033708.

(2) Li, Q.; Kim, K.-S.; Rydberg, A. Lateral Force Calibration of an Atomic Force Microscope with a Diamagnetic Levitation Spring System. *Rev. Sci. Instrum.* **2006**, *77* (6), 065105.

(3) Wang, H. Lateral Force Calibration in Atomic Force Microscopy: Minireview. *Sci. Adv. Mater.* **2017**, *9* (1), 56–64.

(4) Tan, Z.; Wu, Y.; Hong, H.; Yin, J.; Zhang, J.; Lin, L.; Wang, M.; Sun, X.; Sun, L.; Huang, Y.; et al. Two-Dimensional $(C_4H_9NH_3)_2PbBr_4$ Perovskite Crystals for High-Performance Photodetector. *J. Am. Chem. Soc.* **2016**, *138* (51), 16612–16615.

(5) Dou, L.; Wong, A. B.; Yu, Y.; Lai, M.; Kornienko, N.; Eaton, S. W.; Fu, A.; Bischak, C. G.; Ma, J.; Ding, T.; et al. Atomically Thin Two-Dimensional Organic-Inorganic Hybrid Perovskites. *Science (80-.).* **2015**, *349* (6255), 1518–1521.

(6) Holstein, B. R. The van Der Waals Interaction. *Am. J. Phys.* **2001**, *69* (4), 441–449.